J Soils Sediments
DOI 10.1007/s11368-015-1314-0

SEDIMENTS, SEC 1 • SEDIMENT QUALITY AND IMPACT ASSESSMENT • RESEARCH ARTICLE

Heavy metal accumulation reflecting natural sedimentary processes and anthropogenic activities in two contrasting coastal wetland ecosystems, eastern China

Wenhua Gao[1,2] · **Yongfen Du**[1,2] · **Shu Gao**[1,2] · **Jeroen Ingels**[3] · **Dandan Wang**[1,2]

Received: 14 November 2014 / Accepted: 22 November 2015

Abstract
Purpose Due to the impacts of natural processes and anthropogenic activities, different coastal wetlands are faced with variable patterns of heavy metal contamination. It is important to quantify the contributions of pollutant sources, in order to adopt appropriate protection measures for local ecosystems. The aim of this research was to compare the heavy metal contamination patterns of two contrasting coastal wetlands in eastern China. In addition, the contributions from various metal sources were identified and quantified, and influencing factors, such as the role of the plant *Spartina alterniflora*, were evaluated.
Materials and methods Sediment samples were taken from two coastal wetlands (plain-type tidal flat at the Rudong (RD) wetland vs embayment-type tidal flat at Luoyuan Bay (LY)) to measure the content of Al, Fe, Co, Cr, Cu, Mn, Mo, Ni, Sr, Zn, Pb, Cd, and As. Inductively coupled plasma atomic emission spectrometry, flame atomic absorption spectrometry, and atomic fluorescence spectrometry methods were used for metal detection. Meanwhile, the enrichment factor and geoaccumulation index were applied to assess the pollution level. Principle component analysis and receptor modeling were used to quantify the sources of heavy metals.
Results and discussion Marked differences in metal distribution patterns between the two systems were present. Metal contents in LY were higher than those in RD, except for Sr and Mo. The growth status of *S. alterniflora* influenced metal accumulations in RD, i.e., heavy metals were more easily adsorbed in the sediment in the following sequence: Cu> Cd>Zn>Cr>Al>Pb≥Ni≥Co>Fe>Sr≥Mn>As>Mo as a result of the presence and size of the vegetation. However, this phenomenon was not observed in LY. A higher potential ecological risk was associated with LY, compared with RD, except for Mo. Based on a receptor model output, sedimentary heavy metal contents at RD were jointly influenced by natural sedimentary processes and anthropogenic activities, whereas they were dominated by anthropogenic activities at LY.
Conclusions A combination of geochemical analysis and modeling approaches was used to quantify the different types of natural and anthropogenic contributions to heavy metal contamination, which is useful for pollution assessments. The application of this approach reveals that natural and anthropogenic processes have different influences on the delivery and retention of metals at the two contrasting coastal wetlands. In addition, the presence and size of *S. alterniflora* can influence the level of metal contamination in sedimentary environments.

Responsible editor: Gijs D. Breedveld

✉ Yongfen Du
duyongfen@nju.edu.cn

[1] The Key Laboratory of Coast and Island Development of Ministry of Education, Nanjing 210023, China

[2] School of Geographic and Oceanographic Sciences, Nanjing University, Nanjing 210023, China

[3] Plymouth Marine Laboratory, Prospect Place, West Hoe, Plymouth PLI 3DH, UK

Keywords Anthropogenic activities · Coastal wetland · Contamination assessment · Heavy metal sources · Natural sedimentary process · *Spartina alterniflora*

1 Introduction

The transport and accumulation of heavy metals are of great concern in environmental and ecological research because of their inherent toxicity, multiple sources, persistence, and non-

Published online: 16 December 2015

degradability (Wang et al. 2013a; Zhang et al. 2013). Quantifying the contamination and evaluating the relative importance of different pollutant sources are crucial to the management and conservation of wildlife habitats, the maintenance of the ecosystem integrity, and the protection of environmental health for society (Lin et al. 2013). Natural transport processes of heavy metals mainly depend on the presence and transport of fine-grained sediment, which is an efficient sink for heavy metals, with the capacity to concentrate and retain heavy metals which is related to its unique physical (grain size, surface area, and charge) and chemical (composition, cation exchange capacity) properties (Horowitz and Elrick 1987). Furthermore, the bed morphology, hydrodynamic processes, and vegetation in the wetland also influence heavy metal transport and accumulation (Duarte et al. 2010; Zhou et al. 2010; Almeida et al. 2011; Chen and Torres 2012). In addition, rapid industrialization and economic development are accompanied by severe environmental problems (Fang et al. 2012). Anthropogenic processes, such as mining, fossil fuel consumption, and agricultural activities, represent important heavy metal sources (Dietz et al. 2009; Garcia-Tarrason et al. 2013), which contribute significantly to the enhancement of heavy metal contents in coastal wetlands, particularly over the last few decades (Dietz et al. 2009; Garcia-Tarrason et al. 2013; Pisani et al. 2013; Li et al. 2013a, b). It is critical to obtain an improved understanding of the current pollution status and sources of heavy metals in coastal wetlands because of their ultimate relevance to the sustainable development of impacted ecosystems and public health.

Geostatistical methods and techniques, such as the geostatistical methods and techniques, the geoaccumulation index (I_{geo}), and receptor modeling, have long been used to determine the pollution status and the diverse sources of heavy metals. Heavy metal enrichment factor (EF) and I_{geo} are useful in evaluating the anthropogenic influences on the sediment and identifying the sources of heavy metals in riverine, estuarine, and coastal environments (Müller 1979; Zhang and Liu 2002; Feng et al. 2004; Fang et al. 2009; Zhang et al. 2009). Receptor modeling, based on multi-linear regression of the absolute principal component score (MLR-APCS), is also widely used for deriving quantitative estimates of the types and relative importance of the sources (Thurston and Spengler 1985; Song et al. 2006). These methods have been used in research assessing coastal wetland heavy metal pollution status and their controlling factors (Bai et al. 2012; Maanan et al. 2013; Li et al. 2013a, b; Zhang et al. 2013; Hu et al. 2013).

Owing to the differences in tidal processes and the patterns of sediment supply, the coasts in eastern China exhibit spatial variations in tidal flat sedimentation and geomorphology (Gao et al. 2014). For instance, on the coasts to the north of Hangzhou Bay (Fig. 1), huge quantities of sediment supply from the Yellow and Yangtze rivers form thick Holocene sequences on the inner continental shelf, where the coastal water depth is shallow. Thus, wide tidal flats have developed on the coasts of Bohai Bay and northern Jiangsu, forming the low-lying coastal plains (Wang and Zhu 1990). In contrast, to the south of Hangzhou Bay, the coasts are characterized by numerous embayments which are controlled by the various faulting activities. Here, fine-grained particles from the Yangtze River are dispersed towards the south, and the local smaller rivers on the Zhejiang and Fujian coasts also provided some sediment input, which has resulted in the formation of tidal flat systems within the embayments since the late Holocene (Wang and Zhu 1990). In order to compare and identify the heavy metal pollution status and the related sources, we chose two representative tidal flat wetlands (Fig. 1) as our study areas: the Ru Dong wetland (RD) on the Jiangsu coast (located to the north of Hangzhou Bay) characterized by a plain-type tidal flat and the Luoyuan wetland (LY) within a coastal embayment (located to the south of Hangzhou Bay) (Sun et al. 2010; Zhang 2010; Chen 2011; Zhang et al. 2011; Gao et al. 2012; Liao et al. 2012; Li et al. 2012; Yu 2013). A common characteristic of both systems is that the upper part of the wetland has been mostly reclaimed, and the upper intertidal flats are widely covered by the exotic species *Spartina alterniflora* which was introduced to the region in the 1980s. However, they have different ecological features in response to their different geological backgrounds (Wang and Ye 2013; Gao et al. 2014).

Some heavy metals (Zn, Hg, Pb, and Cu) have shown potential biological toxicity in the tidal flats adjacent to the RD area (Li et al. 2012), whereas the contamination level for Cd and As in fishes and crustaceans of the Yellow Sea off the Jiangsu coast is relatively high (Sun et al. 2010). The heavy metal contents in the LY sediments are generally higher than the background values, with Ni and Co being the major pollutants. The LY wetland can be ranked as moderate in terms of the potential ecological risk (Gao et al. 2012), which is related to the coastal industrial distribution and development (Yu 2013). Thus, there are differences in terms of pollution level and the main pollution sources between the RD and LY wetlands. In the present contribution, we (i) compared the differences of the heavy metals between these two systems based on statistical analysis and the receptor model and (ii) identified the sources of heavy metals as well as their influencing factors on heavy metal pollution.

2 Materials and methods

2.1 Study area description and sample collections

The RD wetland (Fig. 1) is located in the northern Yangtze River delta, Jiangsu Province. It lies within the monsoon climate zone, controlled by the alternative oceanic and continental climates during a year. The average temperature is around

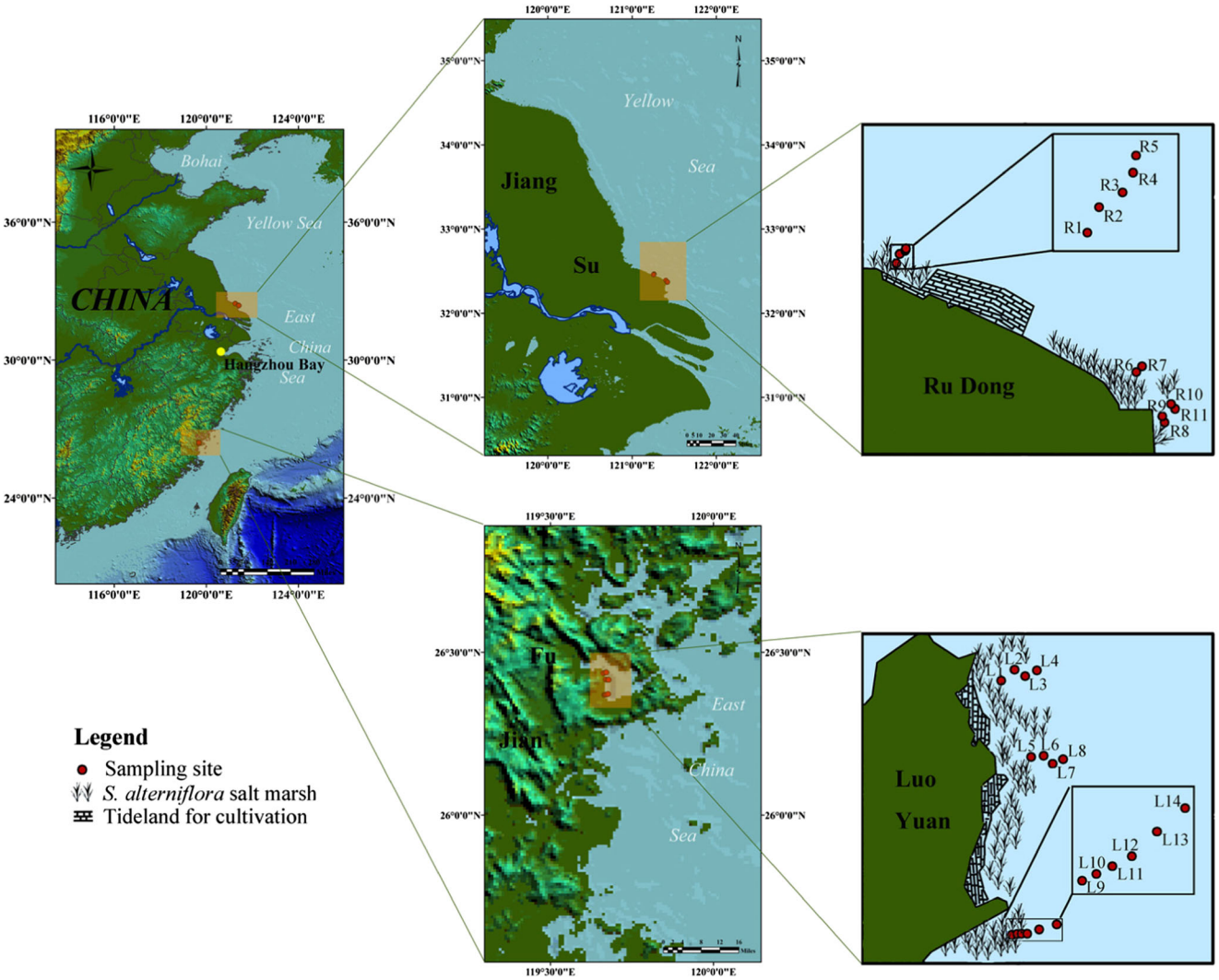

Fig. 1 Location of sampling sites and the surrounding environment of the study area

27.1 °C in July and 17.3 °C in October (Ren 1986). This coast exhibits regular semi-diurnal tides, and tide levels range between minimum 0.21 m and maximum 8.42 m, with an average of 4.61 m; on the tidal flat, the currents are stronger during the flood than during the ebb tide currents (Ren 1986). In addition, the coastal waters are affected by the northern Jiangsu coastal current, Yangtze freshwater discharge, and the Taiwan warm current. The sediment is mostly supplied by the coastal erosion of the abandoned Yellow River delta and the Yangtze River (Wan and Zhang 1985; Li et al. 2001). There are silts and sands in the bare flat, while the bed material is dominated by silts in the *S. alterniflora* salt marshes (Wang et al. 2012).

The LY wetland (Fig. 1) is located on the northeastern Fujian coast, surrounded by the Luoyuan and Huangqi peninsulas. It is a typical semi-enclosed bay caused by tectonic movement. The LY area has a subtropical monsoon climate, with a regular semi-diurnal tide. The average flood and ebb durations are 6.35 and 6.07 h, respectively, with an average tidal range of 4.98 m. The currents within the bay are influenced by the bathymetry/topography. The intertidal zone here is approximately 2–5 km wide, with a gentle tidal flat slope (<0.1 %). The sediment supply originates from external sources, mainly composed of clay–silty materials, which originate from the Yangtze River and a number of small rivers discharging into Zhejiang–Fujian coastal waters, with the former being the major source. The river discharges are transported by the shelf currents towards the study area.

In total, 27 stations were sampled at the RD and LY wetlands (Fig. 1). Eleven sampling stations were located at the RD wetland (R1–R11). Stations R1–R5 were situated along a landward–seaward transect perpendicular to the coastline, whereas R6–R11 were arranged along the coastline. Station R1 was located in the transition zone of *S. alterniflora* and

Table 1 Statistical results of heavy metals in two contrasting coastal wetland ecosystems and the background values (BV) of heavy metals in shallow marine sediment (silts) of the Chinese mainland sediment–shallow marine silt (mg kg^{-1})

	Range	Median	Mean	SD	CV/%	Skewness	Kurtosis	BV
Rudong wetland ecosystem (RD)								
Al	67,588–37,120	58,667	54,672	10,890	19.92	−0.43	−1.40	58,100
Fe	28,902–15,868	24,147	23,743	4110	17.31	−0.66	−0.39	29,000
As	10.06–4.22	5.86	6.68	1.81	27.04	0.62	−0.46	7.30
Cd	0.17–0.06	0.10	0.11	0.04	34.20	0.60	−0.73	0.07
Co	19.13–10.47	16.30	15.79	2.96	18.75	−0.63	−0.78	11
Cr	63.74–28.35	53.21	47.58	12.97	27.26	−0.37	−1.45	60
Cu	12.32–2.60	6.15	6.66	3.30	49.59	0.48	−1.13	15
Mn	617–390	541	529	75	14.17	−0.65	−0.31	540
Mo	11.61–7.77	10.00	10.04	1.11	11.05	−0.29	0.62	0.60
Ni	28.89–15.67	25.34	23.74	4.41	18.57	−0.60	−0.83	23
Pb	8.04–3.24	6.29	6.06	1.52	25.01	−0.54	−0.50	19
Sr	227–128	205	189	34.93	18.47	−0.93	−0.53	222
Zn	110–46	80	76	20.83	27.35	−0.01	−1.20	62
Luoyuan wetland ecosystem (LY)								
Al	76,407–37,299	50,435	52,113	10,936	20.99	0.93	0.62	58,100
Fe	41,115–35,418	39,152	38,456	1888	4.91	−0.45	−1.10	29,000
As	14.92–7.03	7.93	8.65	2.15	24.82	2.24	5.41	7.30
Cd	0.23–0.06	0.10	0.11	0.05	40.92	1.23	1.77	0.07
Co	25.59–21.59	23.51	23.65	1.20	5.06	0.03	−1.00	11
Cr	86.42–63.56	75.48	75.82	6.54	8.62	−0.03	−0.59	60
Cu	22.18–18.74	20.83	20.67	1.19	5.77	−0.17	−1.31	15
Mn	1562–808	1052	1095	255	23.25	0.68	−0.58	540
Mo	3.19–0.05	1.65	1.57	0.90	57.33	−0.02	−0.52	0.60
Ni	45.54–39.38	41.72	42.35	1.96	4.64	0.44	−1.04	23
Pb	26.37–16.21	19.63	19.82	2.98	15.02	0.68	−0.03	19
Sr	98.83–48.71	56.58	60.74	15.11	24.88	1.92	2.92	222
Zn	282–117	155	167	43	25.84	1.49	2.98	62

SD standard deviation, *CV* coefficient of variance

Suaeda glauca, which was inundated only on spring tides. *S. alterniflora* was present in high densities at R2 and R3. Station R4 was located in the transitional zone of *S. alterniflora* and the bare flat. The average height of *S. alterniflora* at R1–R4 was approximately 180 cm at the time of sampling. Station R5 was located on the bare flat, in an area covered with fine sand. In comparison, the R6–11 area was characterized by a patchy distribution of the younger *S. alterniflora* with an average height of 50 cm, with R6, R8, and R10 showing *S. alterniflora* vegetation cover and R7, R9, and R11 lacking vegetation cover, i.e., the bare flat, but lying adjacent to the *S. alterniflora* marsh.

In the LY sampling area, L1–L4, L5–L8, and L9–L12 were arranged in three transects perpendicular to the coastline. Stations L1–L4 were located in the north of the bay. *S. alterniflora* was present at L1 and L2: *S. alterniflora* plants at L1 were about 185 cm high, while younger *S. alterniflora* (90 cm high) plants were found distributed at L2. Station L3 was on the bare flat, but near to the *S. alterniflora* salt marsh.

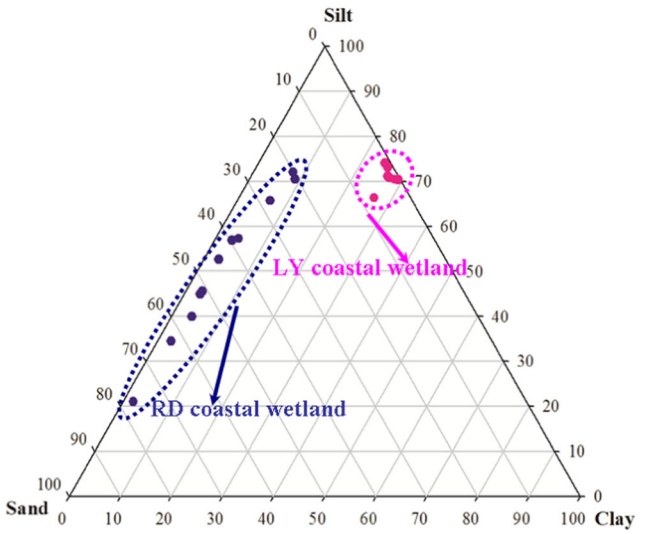

Fig. 2 Percentage (%) contribution of different size fractions of sediments

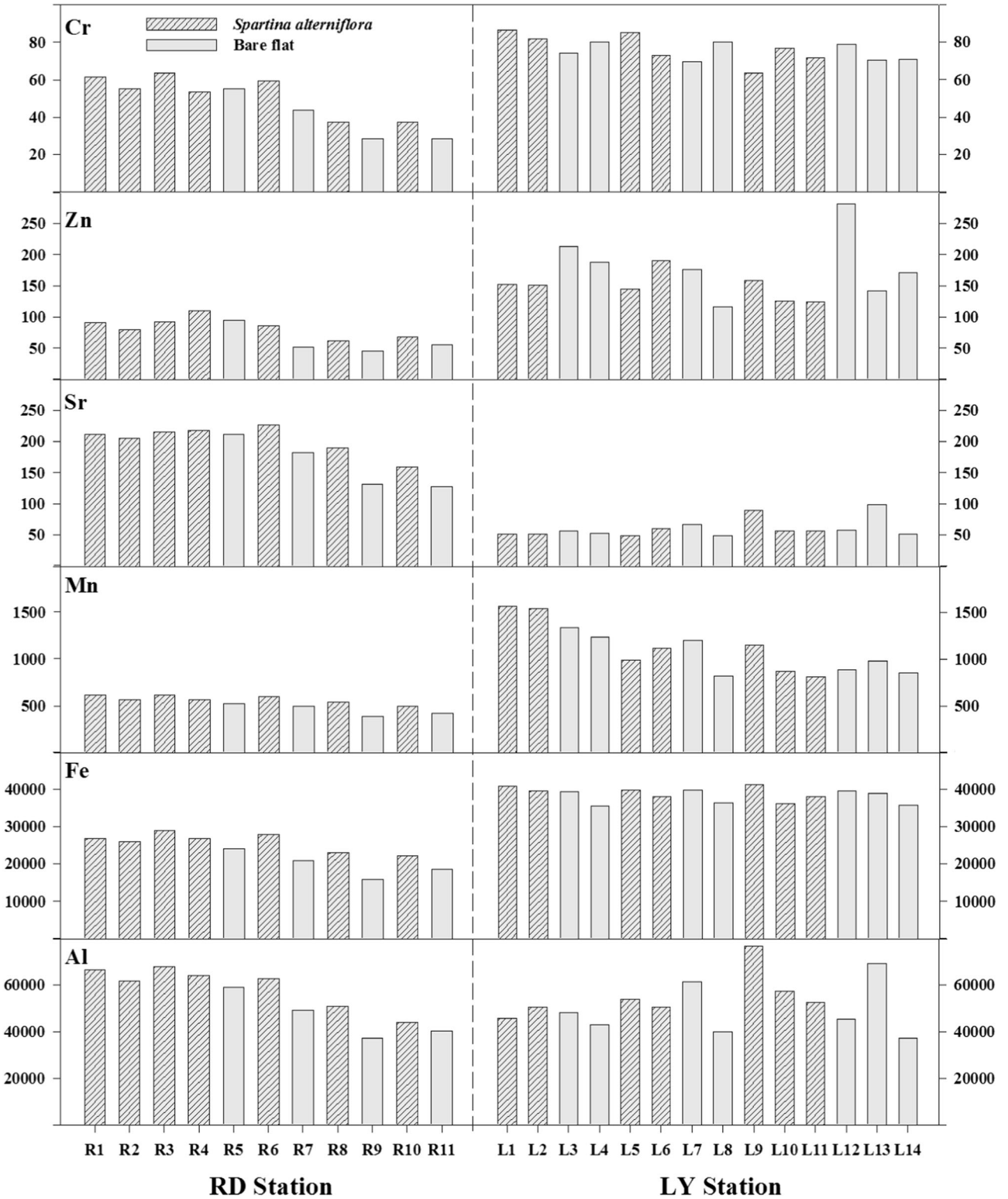

Fig. 3 Heavy metal content variations (mg kg^{-1}) (i.e., Cr, Zn, Sr, Mn, Fe, and Al) in surface sediments from two contrasting coastal wetland ecosystems

Hence, stations L2 and L3 represent the transitional zone between the marsh and the bare flat, with *S. alterniflora* vegetation exhibiting a patchy distribution. Station L4 was also situated on the bare flat, but close to the low water level. The transect L5–L8 lay in the middle of the LY bay; here, *S. alterniflora* plants were present at L5 and L6, while L7 and L8 were on the bare flat. Stations L6 and L7 represented the transitional zone between the *S. alterniflora* vegetation

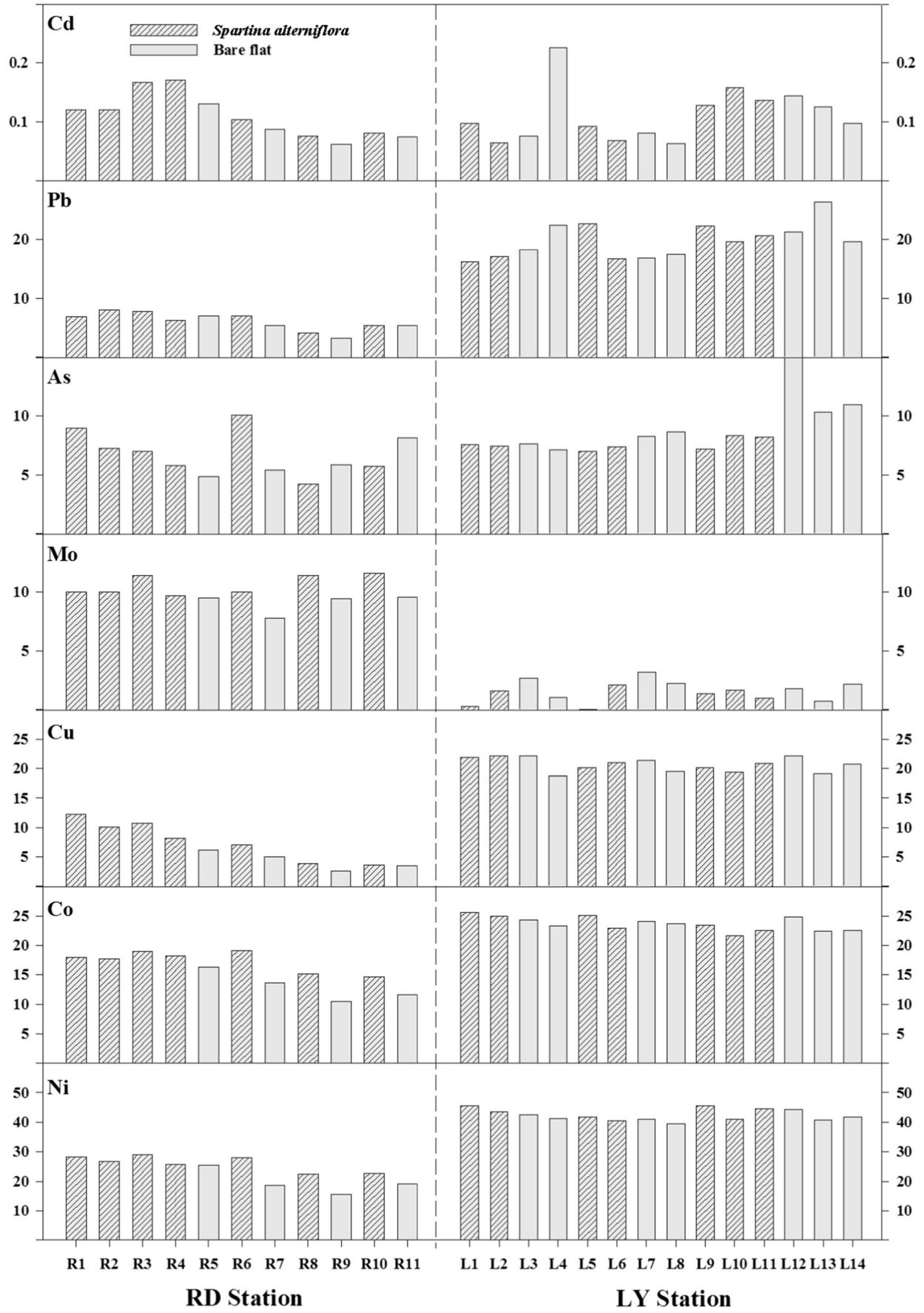
Cd
Spartina alterniflora
Bare flat
Pb
As
Mo
Cu
Co
Ni
R1 R2 R3 R4 R5 R6 R7 R8 R9 R10 R11
L1 L2 L3 L4 L5 L6 L7 L8 L9 L10 L11 L12 L13 L14
RD Station
LY Station

◀ **Fig. 4** Heavy metal content variations (mg kg^{-1}) (i.e., Cd, Pb, As, Mo, Cu, Co, and Ni) in surface sediments from two contrasting coastal wetland ecosystems

and the upper bare flat. Transect L9–L14 was located in the south of the bay. Stations L9–L11 were covered with *S. alterniflora* plants, with plant heights decreasing from L9 to L11, while stations L12–L14 were located on the bare flat.

Samples were taken during ebb tides when the tidal flat was exposed to the air in the period July 9–11, 2010. At each of the stations, four replicate samples were collected by means of modified syringe corers (29-mm internal diameter) to a depth of 8 cm. All the cores were sliced into sub-samples of 2-cm intervals and stored in polyethylene bags at −20 °C, until further analysis in the laboratory.

2.2 Experiments and analyses

2.2.1 Grain size analysis

Sediment grain size was analyzed by using a laser particle size analyzer (Mastersizer 2000, Malvern Instruments Limited, England). For analysis, 1–2 g of sediment sample was placed into a Teflon beaker filled with 20 ml of distilled water, with the addition of ~1 g of sodium hexametaphosphate $(NaPO_3)_6$ to disperse particles; after 24 h of incubation in the $(NaPO_3)_6$ solution, sediment grain size distribution data were obtained using the Mastersizer 2000. Each sample was measured three times, and the relative error of repeated measurements was <3 % (Cheng et al. 2001).

2.2.2 Heavy metal analysis

The analysis of heavy metals was carried out using the acid digestion protocol following Lu (2000). The sample was first dried (105 °C), disaggregated, and ground in an agate mill to pass the mesh size of 100 μm. Then, 0.2 g of the dried sample was digested with 3 ml hydrochloric acid (HCl) and 2 ml nitric acid (HNO_3) in a Teflon reactor (20 min, 80 °C), and the residue was digested further with 5 ml hydrofluoric acid (HF) and 0.25 ml perchloric acid ($HClO_4$) (4 h, 80–100 °C), then heated with 1.5 ml hydrochloric acid, 0.5 ml hydrogen peroxide (H_2O_2), and 3 ml purified water for 2 min, and finally diluted in distilled water for metal measurements.

Concentrations of most metals (i.e., Al, Fe, Co, Cr, Cu, Mn, Mo, Ni, Sr, and Zn) were determined using inductively coupled plasma atomic emission spectrometry (ICP-AES, Optima 5300DV, PerkinElmer, USA). Concentrations of Pb and Cd were measured using flame atomic absorption spectrometry (FAAS, 180-80, Hitachi, Japan). Sample solution was aspirated by a pneumatic analytical nebulizer and transformed into an aerosol, which was then introduced into a spray chamber, where it was mixed with the flame gases and conditioned in such a way that only the finest aerosol droplets enter the flame. Element composition was determined based on the absorption of optical radiation by free atoms in the gaseous state (Broekaert 2005). The element As was measured by using the atomic fluorescence spectrometry (AFS, 610A, Beijing Ruili Analytical Instrument Company, China) method, where the sample material was brought into an atom reservoir and excited by absorbing monochromatic radiation emitted by a primary source. Then, the fluorescence radiation emitted, which may have the same or longer wavelength, was measured (Broekaert 2005).

2.3 Statistical analyses

2.3.1 Enrichment factor

The heavy metal enrichment factor (EF) has been widely used for detecting heavy metal sources and their contamination in riverine, estuarine, and coastal environments (Zhang and Liu 2002; Feng et al. 2004; Fang et al. 2009; Zhang et al. 2009). The EF is commonly defined as the ratio of the observed metal to aluminum (Al) in the sample of interest divided by the background metal/Al ratio, as expressed below (Sinex and Wright 1988):

$$\mathrm{EF} = \frac{(M/\mathrm{Al})_{\mathrm{s}}}{(M/\mathrm{Al})_{\mathrm{B}}} \quad (1)$$

where $(M/\mathrm{Al})_{\mathrm{s}}$ is the metal to Al ratio in the sample and $(M/\mathrm{Al})_{\mathrm{B}}$ is the natural background metal to Al ratio. As Al is one of the most abundant elements on Earth and poses no concern for contamination risk, it is therefore commonly used for normalization purposes (Zhang et al. 2009). The background values (Table 1) utilized here are the contents of heavy metals of shallow marine sediment (silt) from the Chinese mainland (Zhao and Yan 1994).

In terms of the assessment criteria, EF values <0.5 reflect mobilization and loss of these elements relative to Al, or indicate an overestimation of the reference metal contents (Zhang 1995). If the values lie between 0.5 and 1.5, then the trace metals may be entirely from crustal materials or natural weathering processes; a value >1.5 implies that a significant portion of the trace metal originates from non-crustal material (Zhang and Liu 2002). According to Han et al. (2006), contamination determination is classified into two categories: EF≤ 2 suggests a deficiency of minimal metal enrichment, while EF>2 indicates metal enrichment.

2.3.2 Geoaccumulation index

The geoaccumulation index (I_{geo}), which was initially introduced by Müller (1979), is used to define metal contamination

in sediments by comparing the present-day concentrations with pre-industrial levels:

$$I_{\text{geo}} = \log_2\left(\frac{C_n}{1.5B_n}\right) \quad (2)$$

where C_n is the measured heavy metal content in the sediment (n refers to the metal) and B_n is the background content of the same heavy metal (n). The constant 1.5 in the denominator is the background matrix correction factor related to lithogenic effects, whereas the background values of heavy metals of interest are the same as those used in the EF calculation outlined above (Table 1). Seven classes are distinguishable for the geoaccumulation index from class 0 ($I_{\text{geo}} \leq 0$) to class 6 ($I_{\text{geo}} > 5$) (Müller 1979); class 6 represents at least a 100-fold enrichment above the background values.

2.3.3 Principle component analysis

Principle component analysis (PCA) is a powerful technique for pattern recognition that attempts to explain the variance of a large set of inter-correlated variables and transform them into a smaller set of independent (uncorrelated) variables (principal components, PCs). The first step in this analysis is to transform the elemental data into a dimensionless standardized form:

$$C_{ij} = \frac{\left(c_{ij} - \overline{c}_i\right)}{\sigma_i} \quad (3)$$

where i is the total number of elements, j is the sample number, c_{ij} is the concentration of element i in sample j, and $\overline{c}_i$ and σ_i are the arithmetic mean concentration and the standard deviation for element i, respectively. The PCs are expressed as (Singh et al. 2005):

$$z_{kj} = a_{k1}C_{1j} + a_{k2}C_{2j} + a_{k3}C_{3j} + \cdots + a_{ki}C_{ij} \quad (4)$$

where z is the component score, a is the component loading, C is the dimensionless standardized concentration of the element, and k is the component number. The situations of factor loading >0.75, for both positive and negative correlations, were taken into account (Retnam et al. 2013). For the analytical procedure, PCA was conducted using the software SPSS 13.0.

2.3.4 Receptor modeling

Receptor modeling, based on multi-linear regression of the absolute principal component score (MLR-APCS), is a widely employed statistical technique for deriving quantitative estimates of source contributions and source profiles (Thurston and Spengler 1985). Firstly, in order to normalize data of PCA results, the "absolute zero" PC score was introduced and estimated for each PC wherein all the elemental concentrations are zero. This was accomplished by deriving the Z-score for absolute zero concentrations as follows.

$$(Z_0)_i = \frac{0 - \overline{c}_i}{\sigma_i} = -\frac{\overline{c}_i}{\sigma_i} \quad (5)$$

Then, regression was used to derive the source contributions, which is expressed as:

$$M_j = \zeta_0 + \sum_{k=1}^{p} \zeta_k \text{APCS}^*_{kj} \quad (6)$$

where M_k is the measured mass contents in sample j. In the equation, APCS^*_{kj} denotes the rotated absolute component score for source k in sample j; thus, $\zeta_k\text{APCS}_{kj}$ represents the mass contribution in sample j made by source k. ζ_0 is the contribution made by sources that are not included in the PCA. Finally, the source profiles were obtained from the regression between c_{ij} and $\zeta_k\text{APCS}_{kj}$. Using this, the source contributions to individual species can be calculated from the source profiles and the mass contributions (Song et al. 2006).

3 Results

3.1 Sediment grain size

The different size fractions of the sediments from RD and LY are shown in Fig. 2. In RD, sand and silt represent the major components at almost all sampling sites, with the clay content <10 %. Sand content increased gradually from land towards

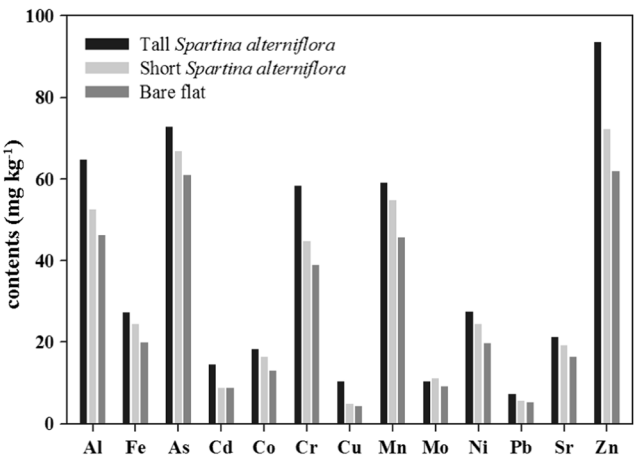

Fig. 5 Heavy metal distributions in the sediment from tall *Spartina alterniflora* (TSA) salt marsh, short *S. alterniflora* (SSA) salt marsh, and bare flat (BF) in the RD coastal wetland. (Contents: Fe and Al× 1000; As/10; Cd/100; Mn×10; Sr×10)

the sea (i.e., from R1 to R5), reaching a maximum at R5. However, at all the LY sampling stations, silt proportions were highest, followed by the clay (24–29 %) and sand (0.34–2.47 %) fractions. These different sediment compositions indicate that the RD and LY wetland ecosystems are substantially different in terms of depositional environment.

3.2 Heavy metal accumulation

3.2.1 Heavy metal accumulation in the sediments

The summary statistics for heavy metals are shown in Table 1. Most heavy metals at both coastal wetlands exceeded the respective regional background values of the shallow marine silt deposits, except for Fe, Cu, and Pb in the RD wetland and Sr at LY. At RD, all coefficient of variation (CV) values exceeded 10 % (11.05–49.57 %), indicating a large variability in heavy metal accumulations at the different RD stations. Similarly, some heavy metals (e.g., Cd and Mo) also showed large variability between the different sampling stations at LY (CV values >40 %). However, some other heavy metals (e.g., Fe, Co, Cr, Cu, and Ni) showed less variability between the sampling sites (CV values <10 %) at LY.

As illustrated in Figs. 3 and 4, there were large differences in heavy metal contents between the two coastal wetlands. Most heavy metals (e.g., Fe, Mn, Zn, Cr, Pb, Cu, Co, and Ni) were more abundant in the LY sediments compared to the RD sediments, especially for Mn, Pb, and Cu, for which the sediment accumulation was over twice the value observed in the RD sediments. However, some heavy metals (e.g., Sr and Mo) were much less abundant in the LY sediment compared to the RD sediments. The sediment heavy metal content of other metals, such as Al, Cd, and As, did not exhibit any clear differences between RD and LY.

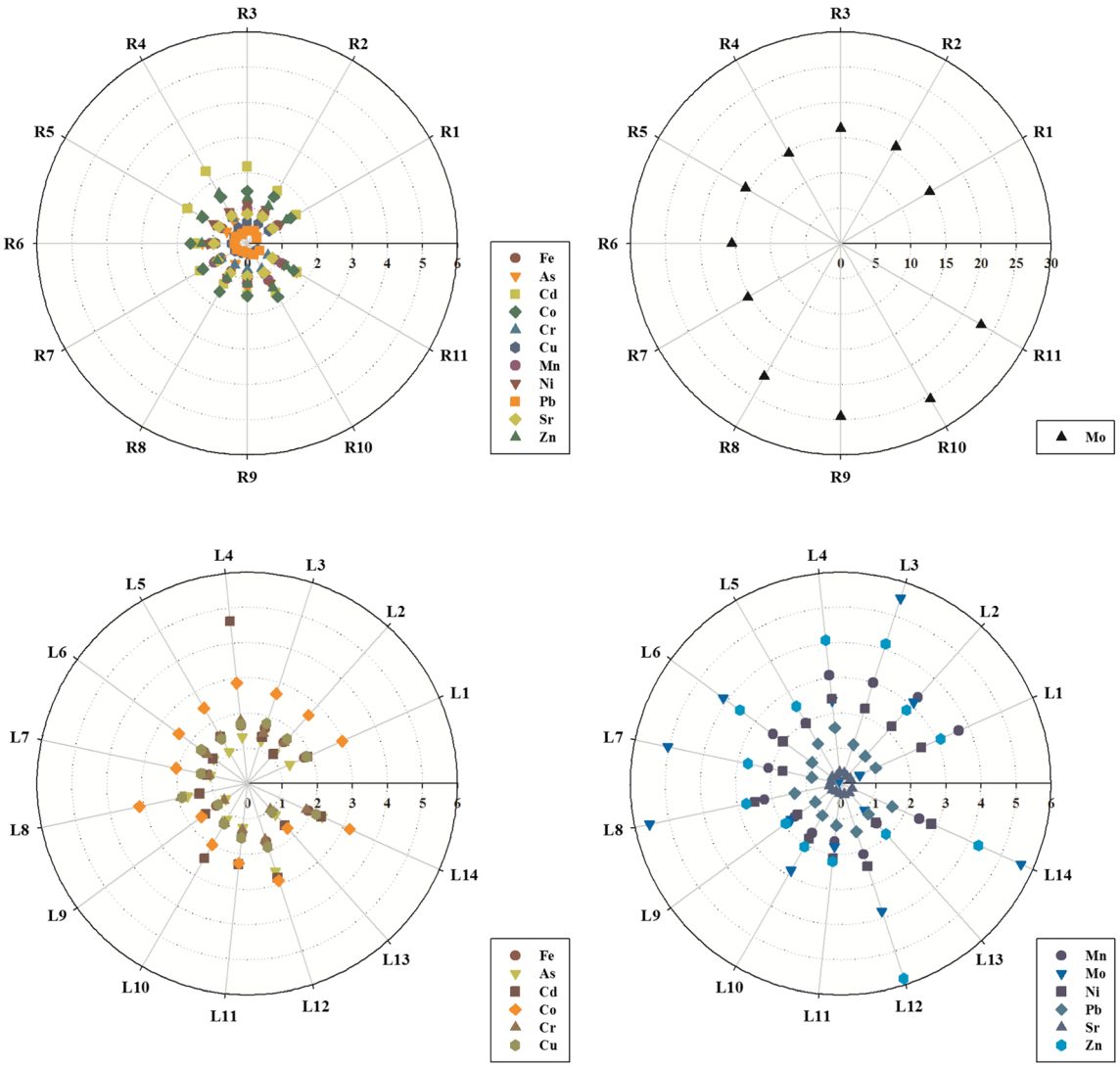

Fig. 6 Polar plot of heavy metal enrichment factor values in the sediments in both coastal wetland ecosystems (*R* represents Rudong (RD) coastal wetland; *L* is Luoyuan (LY) coastal wetland)

At each coastal wetland, certain heavy metals displayed a uniform accumulation pattern (e.g., Mn and Pb at RD; Sr, Fe, Cu, Co, and Ni at LY), whereas other metals exhibited a large variation among the sites. Along the transects perpendicular to the shoreline (i.e., R1–R5 in RD; L9–L14 in LY), some heavy metal contents decreased towards the sea (e.g., for As and Cu in RD; Cd in LY), but this was not a general trend. Along the coastline, the sediment content values of most heavy metals at the RD wetland decreased from north to the south, except for Zn, As, and Mo. However, this pattern was not observed for the LY stations, except for Mn.

3.2.2 Comparison of heavy metal accumulation between the S. alterniflora salt marsh and the bare flat

At the RD coastal wetland, heavy metals in the *S. alterniflora* salt marsh sediments exhibited greater accumulation levels than in the bare flat sediments (Figs. 3 and 4). Differences were also present between the tall *S. Alterniflora* (TSA) salt marsh, the short *S. alterniflora* (SSA) salt marsh, and the bare flat (BF) at the RD coastal wetland (Fig. 5). For most heavy metals, the TSA salt marsh sediments contained the highest concentrations, followed by the SSA salt marsh and the BF sediments. However, this trend was not observed for Pb, Cd, and Cu. The element Mo showed a different accumulation pattern compared to the other heavy metals, with the highest concentrations observed in the SSA salt marsh. Generally, however, our observations indicate that the growth condition (i.e., size) of *S. alterniflora* is an important influencing factor for heavy metal accumulation.

The heavy metal contents at LY showed complex variations between *S. alterniflora* salt marshes and the bare flat (Figs. 3 and 4). There were no differences in accumulation patterns between the *S. alterniflora* salt marsh and the bare flat for Fe, Cu, Co, and Ni. For other heavy metals, accumulation levels at *S. alterniflora* stations were greater than those at the bare flat, but the reverse trend was also found.

3.3 Contamination assessment

The EF values of most heavy metals at LY were higher than those at RD except for Mo (Fig. 6), indicating a generally higher contamination level at LY compared to RD. The higher EF value of Mo at RD suggests a specific anthropogenic impact in this area. In addition, the EF values for Cd at R3 and R4 were greater than that of R2, implying significant Cd contamination at these two sites. At LY, the EF values of most heavy metals (except for Fe, Cr, Pb, and Sr) were >2, indicating a high degree of heavy metal contamination in this area.

The I_{geo} values for the RD wetland were generally <0 (except for Cd, Co, and Mo), suggesting low contamination levels (Fig. 7), but the I_{geo} value of Mo here was >3, indicating a moderate Mo pollution. At LY, Cd, Co, Mn, Mo, Ni, and Zn I_{geo} values were >0, with Mo and Zn values >1, implying that Mo and Zn contribute most to heavy metal pollution in this area (Fig. 8).

4 Discussion

4.1 Heavy metal sources in the two coastal wetlands

The PCA and receptor modeling (MLR-APCS) were used to identify the sources of heavy metals for the two coastal wetland systems. The PCA generated three PCs for RD and four PCs for LY, with an eigenvector >1, explaining 92.4 % (RD)

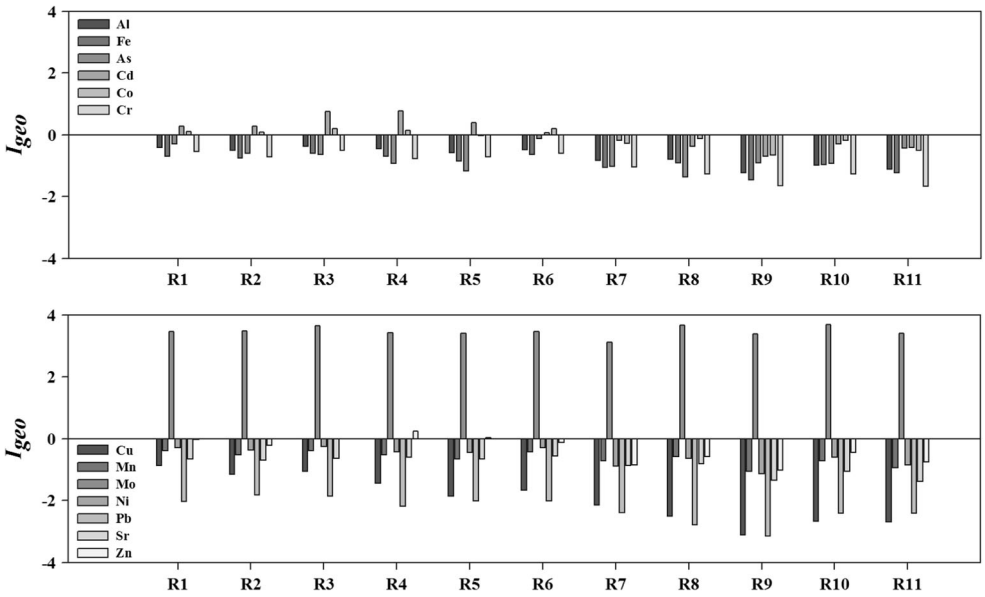

Fig. 7 Heavy metal geoaccumulation index (I_{geo}) in surface sediments from Rudong coastal wetland (RD)

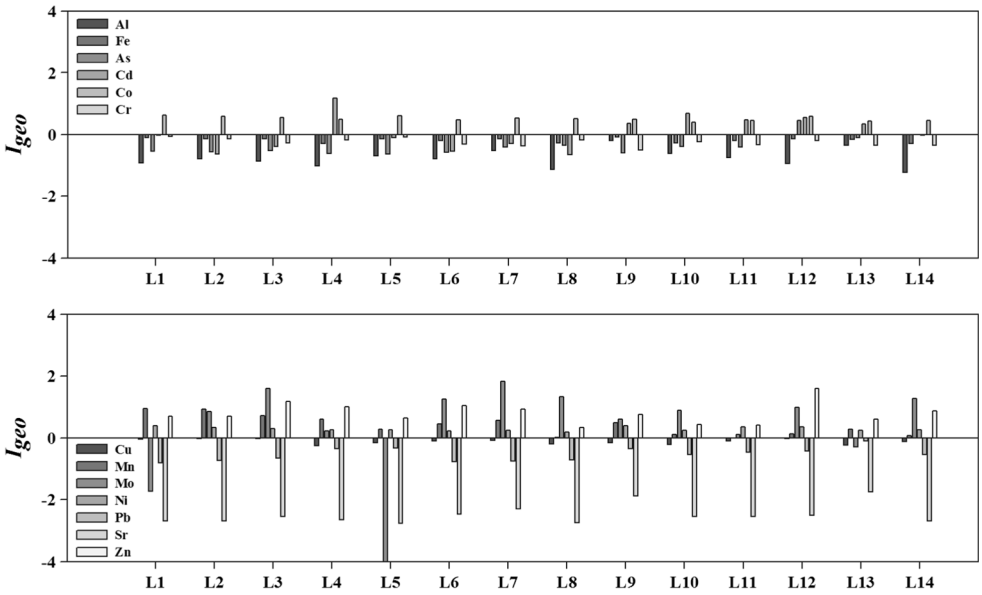

Fig. 8 Heavy metal geoaccumulation index (I_{geo}) in surface sediments from Luoyuan coastal wetland (LY)

and 83.3 % (LY) of the total variance in the heavy metal data sets. The corresponding sources, together with the variable loadings and variances explained, are listed in Table 2.

For the RD data set, PC1 (explaining 60.75 % of the total variance) had strong positive loadings (>0.80) of Al, Fe, Cd, Co, Cr, Cu, Mn, Ni, Pb, Sr, and Zn. Based on their EF values, these heavy metal concentrations are lower than or close to their background values in the region, except for Cd, Co, Ni, and Zn, suggesting that the majority of these heavy metals are mainly controlled by natural sedimentary processes. Therefore, PC1 in the RD coastal wetland can be seen as representative of natural source factors. PC2 (explaining 12.45 % of total variance) has strong positive loadings for As. There is an extremely small amount of As in the natural environment, but it is an important component of chemical fertilizers and insecticides. There is a large number of farming activities in the coastal area, and it has been reported that fermented chicken manure is being used for aquaculture ponds, which enriches the coastal water masses since the wastewater is discharged from the ponds (Liu et al. 2013). Thus, PC2 is here assumed to represent the agriculture impact on heavy metals at the RD coastal wetland. PC3 has strong positive loadings for Mo, which can be interpreted as an industrial source, because Mo is the important raw material in the local industry.

For the LY coastal wetland, four main sources of heavy metals were identified by the PCA analysis. Among these four, PC1 explained 26 % of total variance and had strong positive loadings of Fe, Co, Cu, Mn, and Ni. These heavy metal contents were all beyond the background values, and both the EF and I_{geo} values were relatively high, indicating that anthropogenic activities can be associated with this PC1 axis. There are many factories that use iron, steel, and nickel around the LY coastal area. Therefore, PC1 was assumed to represent industrial sources. PC2, explaining about 23 % of total variance, had strong positive loadings of the metals Al and Sr and a negative loading for Cr. Al and Sr in the LY coastal area were both lower than the background values, and PC2 was hence assumed to represent the influence of natural sedimentary processes. PC3 had strong positive

Table 2 Loadings of heavy metals on significant principal components for the Rudong and Luoyuan (RD and LY) coastal wetlands

	RD coastal wetland			LY coastal wetland			
	PC1	PC2	PC3	PC1	PC2	PC3	PC4
Al	*0.97*	0.20	0.07	0.20	*0.89*	0.18	−0.24
Fe	*0.92*	0.22	0.28	*0.89*	0.37	−0.09	−0.01
As	0.15	*0.97*	−0.02	−0.13	0.01	0.13	*0.89*
Cd	*0.92*	−0.09	−0.02	−0.25	0.01	*0.77*	0.19
Co	*0.93*	0.22	0.25	*0.81*	−0.41	−0.12	0.07
Cr	*0.94*	0.26	0.01	0.29	*−0.86*	0.21	−0.15
Cu	*0.83*	0.38	0.00	*0.66*	−0.18	*−0.54*	0.39
Mn	*0.87*	0.26	0.29	*0.72*	−0.13	−0.22	−0.29
Mo	0.11	−0.03	*0.98*	−0.34	0.13	*−0.81*	0.32
Ni	*0.88*	0.31	0.33	*0.75*	0.11	0.22	0.20
Pb	*0.82*	0.40	−0.02	−0.17	0.42	*0.80*	0.13
Sr	*0.95*	0.06	0.05	0.04	*0.93*	0.22	0.01
Zn	*0.91*	0.00	0.11	0.25	−0.07	−0.09	*0.85*
Total	9.07	1.62	1.32	3.38	2.96	2.46	2.03
% of Variance	69.75	12.45	10.19	26.00	22.80	18.90	15.60
Cumulative %	69.75	82.20	92.39	26.00	48.80	67.70	83.30

Italicized values represent strong loadings

loadings of both Cd and Pb, but strong negative loadings of Cu and Mo, potentially representing traffic and emission sources, since Pb has been widely used as an antiknocking additive in petrol (Prosi 1989) and can persist in soils and sediments for decades. However, considering the widespread use of Pb in many industrial activities, we cannot exclude industrial contributions to PC3 in this case. PC4 had strong positive loading for As and Zn, representing an agriculture source because there is an extremely small amount of As in the natural environment and As and Zn are both important components of chemical fertilizers and insecticides.

The PCA results together with the EF and I_{geo} values suggest that heavy metals in both wetlands are strongly influenced by natural sedimentary processes, agricultural input, industrial activities, and traffic vehicle emissions. Quantification of contributions from the different sources of heavy metals, based on receptor modeling results from MLR-APCS for source apportionment, is presented in Table 3. Multiple regression results indicated very close agreement between the estimated and measured mean values. The relative contributions of different sources of heavy metals are shown in Figs. 9 and 10. For the RD coastal wetland, most of the heavy metal sources were attributed to the natural sedimentary environment to a large degree, with contributions between 3.89 % (Mo) and 80.18 % (Cr). A few heavy metals, like Mo and As, could be ascribed to industrial sources (93.57 % for Mo) and agriculture activities (71.35 % for As). Some other sources that contributed to heavy metal accumulations, especially for Cd (48.03 %) and Sr (31.23 %), were not identified by the methods used here. The situation was quite different at LY. Most of the contributions were distributed along the axis of industrial activities, agriculture activities, and traffic vehicle emissions. Most heavy metals, such as Fe, Co, Cr, Cu, Mn, and Ni, were contributed by local industrial activities

Table 3 Source contribution for each heavy metal in Rudong and Luoyuan (RD and LY) coastal wetlands using receptor modeling results from multi-linear regression of the absolute principal component score (MLR-APCS)

Parameters	Source type				Estimated mean (E)	Observed mean (O)	R^2
	S1	S2	S3	S4			
RD coastal wetland							
Al	63.44	10.87	12.06	–	54,671.91	54,671.84	0.98
Fe	52.43	10.61	42.36	–	23,743.36	23,743.42	0.98
As	13.62	71.35	–	–	6.68	6.68	0.96
Cd	51.97	–	–	–	0.11	0.11	0.85
Co	56.90	11.10	40.42	–	15.80	15.79	0.97
Cr	84.12	18.98	1.81	–	47.55	47.58	0.96
Cu	135.79	52.02	–	–	6.65	6.66	0.84
Mn	40.63	10.15	35.45	–	529.55	529.43	0.92
Mo	3.89	–	93.57	–	10.04	10.04	0.98
Ni	53.80	15.71	53.16	–	23.75	23.74	0.99
Pb	67.46	27.19	–	–	6.06	6.06	0.83
Sr	57.54	2.82	8.41	–	189.12	189.10	0.90
Zn	81.56	0.21	26.84	–	76.18	76.15	0.85
LY coastal wetland							
Al	18.59	–	88.00	17.27	52,112.64	52,112.59	0.92
Fe	1.83	–	89.79	–	38,456.29	38,456.44	0.94
As	0.31	175.40	–	14.87	8.65	8.65	0.83
Cd	0.49	61.91	–	145.74	0.11	0.11	0.69
Co	–	2.70	84.12	–	23.65	23.65	0.85
Cr	–	–	50.89	8.24	75.79	75.82	0.89
Cu	–	17.74	77.39	–	20.66	20.67	0.91
Mn	–	–	344.60	–	1095.00	1095.09	0.69
Mo	7.25	140.76	–	–	1.59	1.57	0.89
Ni	0.52	7.42	71.49	4.75	42.35	42.35	0.67
Pb	6.35	15.91	–	56.09	19.82	19.82	0.87
Sr	22.97	1.26	20.77	24.84	60.74	60.74	0.91
Zn	–	173.85	134.51	–	166.86	166.73	0.79

S1 natural sedimentary processes, *S2* agriculture activities, *S3* industrial activities, *S4* traffic vehicle emission

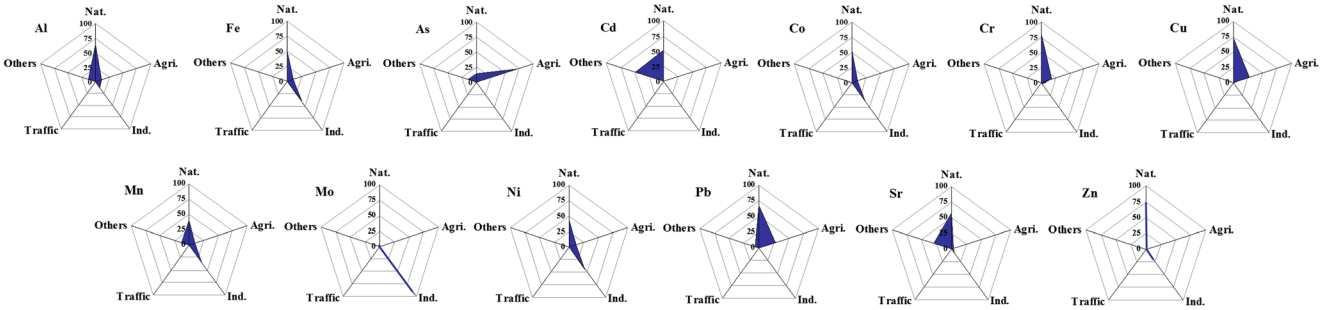

Fig. 9 Source contributions for heavy metals in the Rudong coastal wetland (RD) based on receptor modeling results from multi-linear regression of the absolute principal component score (MLR-APCS)

with a contribution rate of more than 50 %. Other heavy metals (i.e., As and Mo) were derived from agriculture activities, accounting for 92 and 95 % of their presence, respectively. Traffic vehicle mission is mostly linked to Cd (70 %) and Pb (56 %). Natural sedimentary processes also contributed to heavy metal concentrations in the area, but the contribution rate is <20 %, so there are other sources of heavy metal pollution in this area. Overall, heavy metals from the RD coastal wetland were jointly influenced by natural sedimentary processes and anthropogenic activities, whereas in the LY coastal wetland, the heavy metal sources are dominated by anthropogenic activities.

4.2 Effect of sedimentary environment on heavy metal accumulation

One of the most important factors regulating element availability in salt marsh ecosystems is the hydrodynamics which govern sediment transport and vegetation zonation as well as a variety of physical, chemical, and biological processes (Williams et al. 1994). Meanwhile, hydrologic processes are closely related to the seabed morphology of the coastal area, which also affects the variability of metal accumulation within the coastal area (Du Laing et al. 2009).

The RD coastal wetland is located on the Jiangsu coast, an open coastal zone, consisting of a huge tidal flat plain and wide intertidal zone. In the last 2000 years, due to the large quantities of sedimentary materials supplied from the Yangtze and Yellow Rivers, large-scale lowland plains were formed, and its area is now greater than 20,000 km^2. A radial sand ridge field is located off the shore, covering an area of 25,000 km^2. Meanwhile, large-scale tidal flats are formed, with an area of >5000 km^2, and their width is generally >10 km. The prograding tidal flat from land to sea typically consists of salt marsh, mud flat, and silt/sand flat (Ren 1986). This type of tidal flat provides ideal conditions for material exchange between sea water and the sediments. Salt marsh sediments are periodically inundated by saline water during high tides, and this water mass slowly leaches out as groundwater at low tide. In the mud flat and lower marsh areas, which are flooded for prolonged periods, the groundwater table is at or near the sediment surface. When sediment layers are exposed under oxygenated conditions, stable phases of metals are the most adsorbed species. Important adsorbing phases are Fe/Mn hydroxides, carbonates, organic matter, and clay minerals. Waterlogging of salt marsh sediments restricts atmospheric oxygen diffusion into the sediment and thus promotes the development of anoxic sediment, which plays major roles in the potential flux of metals from sediment to surface water (Du Laing et al. 2009). This is a reason for the metal content to decrease from land towards the sea. In addition, significant positive correlations between elements and clay-size sediments at RD (Table 4) suggest that the local fine-size sediment plays an important role in the metal accumulation at the RD

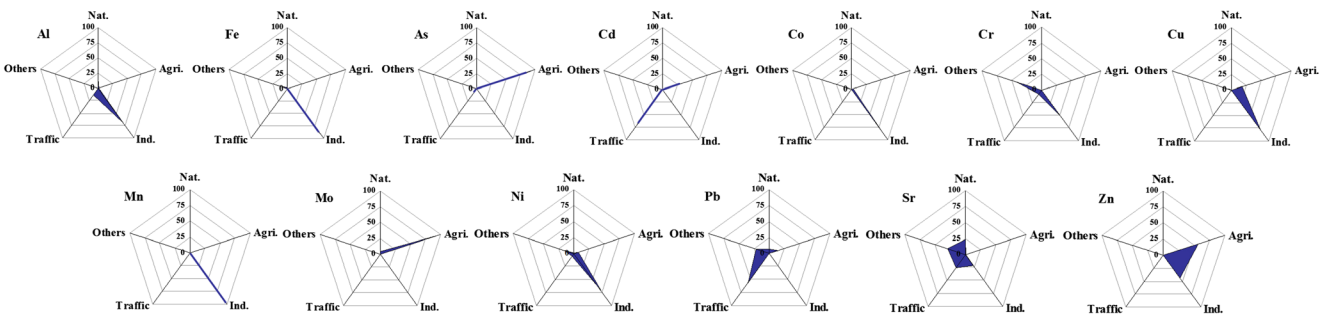

Fig. 10 Source contributions for heavy metals in the Luoyuan coastal wetland (LY) based on receptor modeling results from multi-linear regression of the absolute principal component score (MLR-APCS)

Table 4 Pearson correlation (PC) coefficients between the elements and the grain size fractions in the Rudong and Luoyuan (RD and LY) coastal wetlands

	Al	Fe	As	Cd	Co	Cr	Cu	Mn	Mo	Ni	Pb	Sr	Zn
RD coastal wetland													
Clay	0.66*	0.61*	0.47	0.52	0.60*	0.63*	0.88**	0.63*	0.19	0.64*	0.66*	0.46	0.44
Silt	0.30	0.30	0.45	0.31	0.27	0.27	0.62*	0.32	0.20	0.33	0.38	0.05	0.19
Sand	−0.35	−0.34	−0.46	−0.34	−0.32	−0.32	−0.66*	−0.37	−0.20	−0.37	−0.42	−0.10	−0.22
LY coastal wetland													
Clay	−0.05	0.24	−0.51	0.14	0.41	0.29	0.25	0.69**	−0.03	0.47	−0.37	−0.29	0.08
Silt	0.07	−0.07	0.45	0.38	−0.28	−0.25	−0.02	−0.05	−0.25	0.37	0.51	0.38	0.12
Sand	−0.12	−0.05	−0.16	−0.46	0.13	0.15	−0.05	−0.26	0.25	−0.59*	−0.32	−0.27	−0.12

* correlation is significant at the 0.05 level (two-tailed); ** correlation is significant at the 0.01 level (two-tailed)

coastal wetland, because the smaller particles (as opposed to larger particles) have a larger surface area to volume ratio and are able to adsorb metals in the sediment (Zhang et al. 2002).

The type of sedimentary environment (i.e., coastal plain tidal flat) at RD is favorable for both metal accumulation and salt marsh plant growth (e.g., *S. alterniflora*). The growth of *S. alterniflora* can have a substantial effect on heavy metal accumulation in the sediments of the coastal area (Zhang et al. 2014). Comparison of the heavy metal contents ratio between tall *S. alterniflora* (TSA)/bare flat (BF) and short *S. alterniflora* (SSA)/bare flat clearly demonstrates the greater heavy metal retention for TSA for all metals, except for Mo (Fig. 11). It has been confirmed that *S. alterniflora* is a tolerant plant, with more Cu being retained in the roots to provide suitable conditions for its various important metabolic activities, including photosynthesis in the aboveground parts (Chai et al. 2014). In addition, the high tolerance of *S. alterniflora* with regard to other metals (e.g., Cd, Pb, Hg, and Zn) has been reported by Li et al. (2013a). The capacity of *S. alterniflora* to promote metal adsorption in the sediments varies greatly between different heavy metals: Cu>Cd>Zn>Cr>Al>Pb≥Ni≥Co>Fe>Sr≥Mn>As>Mo. Metal tolerance mechanisms in plants are attributed mainly to compartmentation, metal excretion, and chelation (Tomsett and Thurman 1988; Prasad 1997; Gomez 2013).

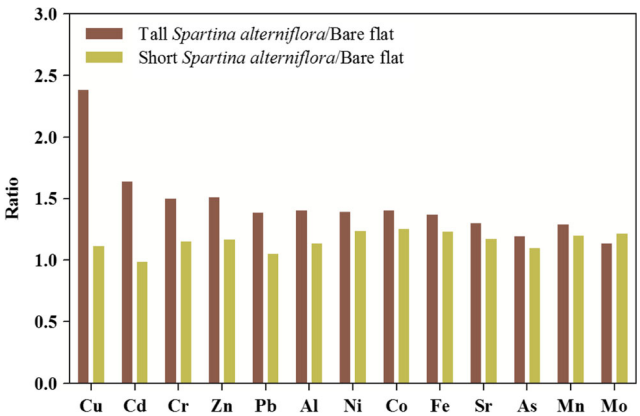

Fig. 11 Ratios of different elements between tall *Spartina alterniflora* and bare flat or between short *S. alterniflora* and bare flat

In contrast, the LY coastal wetland is a typical semi-closed bay (geologically controlled, embayment-type tidal flat). The LY wetland is relatively narrow compared to the RD wetland. As a result, the slope of the tidal flat is comparatively large. The sediment here is mainly supplied externally (e.g., Yangtze River sediment carried by shelf currents) and by the local small rivers. A residual circulation is present within the embayment, which is controlled by tidal processes and the seabed bathymetry. Land reclamation has been undertaken in the upper tidal flat, together with cultivation activities beyond the sea dyke (Wang and Ye 2013). The narrow tidal flat and weak tidal currents reduce the intensity of sediment–seawater interaction.

Some studies have indicated that in the *S. alterniflora* salt marsh at LY, the surficial sediment often erodes at the early stage of flood tide and at the late stage of ebb tide (Wang and Ye 2013). Meanwhile, typhoons occur frequently here in summer, enhancing the turbulent kinetic energy and bottom shear stress greatly and causing intense erosion during the typhoon events. The erosion flux during the whole tidal cycle can reach 40 kg m^{-2}. After the typhoon events, the bottom shear stress decreases gradually, leading to deposition of the suspended sediment (Wang and Ye 2013). Another study reported that during a single typhoon event, the sediment layer formed in a 2-year period could be eroded (Wang et al. 2013b). A new sediment layer will form after the typhoon events, which could redistribute the metals and change their fates in the sediments. Thus, typhoons can modify and create the sediment (re)deposition, which further influences the element delivery and accumulation processes.

5 Conclusions

Marked differences in heavy metal distribution patterns were found between the two coastal wetland systems. The

sedimentary metal contents associated with the embayment-type tidal flat (e.g., LY) were generally higher than those for a low-lying coastal plain tidal flat (e.g., RD) except for Sr and Mo. The presence of *S. alterniflora* had a strong influence on the accumulation of heavy metals in the RD area, but this was less significant in the LY area.

At RD, the presence and growth status of the *S. alterniflora* vegetation influenced the metal accumulation; the presence of *S. alterniflora* caused greater heavy metal accumulation compared to the bare flats, and tall vegetation caused greater heavy metal accumulation than small vegetation. In addition, heavy metals were more easily adsorbed in the sediment in the following sequence: Cu>Cd>Zn>Cr>Al>Pb≥Ni≥Co>Fe>Sr≥Mn>As>Mo, under the influence of *S. alterniflora*. However, this phenomenon is not observed at LY.

The LY coastal wetland faces a higher potential ecological risk than the RD coastal wetland, except for Mo; Mo pollution is serious in the RD coastal wetland. Based on the receptor model output, the heavy metal accumulation at the RD coast is jointly influenced by natural sedimentary processes and anthropogenic activities, whereas it is dominated by anthropogenic activities at the LY coastal wetland.

The type of sedimentary environment determines the fate of metals in the sediment; the plain-type tidal flat is a favorable environment with great potential for material exchanges. However, such interactions are relatively weak for narrow, coastal embayment-type tidal flats, although typhoon events may modify and create new sediment accumulation conditions, which in turn influence the element delivery and accumulation processes.

Acknowledgments This research was supported by the Ministry of Science and Technology of China (2013CB956504) and the National Natural Science Foundation of China (40906066). J. Ingels was supported by a Plymouth Marine Laboratory (PML) Postdoctoral Fellowship and a Marie Curie Intra-European Fellowship within the 7th European Community Framework Programme (Grant Agreement FP7-PEOPLE-2011-IEF No 300879). We gratefully acknowledge Drs. Charles Nittrouer and Andrea Ogston, and anonymous reviewers, for their constructive comments on the original manuscript. Thanks are also due to Longhui Zhang and Deli Wu for their assistance in field sample collection and some previous work in laboratory.

References

Almeida CMR, Mucha AP, Vasconcelos MT (2011) Role of different salt marsh plants on metal retention in an urban estuary (Lima estuary, NW Portugal). Estuar Coast Shelf Sci 91:243–249

Bai JH, Xiao R, Zhang KJ, Gao HF (2012) Arsenic and heavy metal pollution in wetland soils from tidal freshwater and salt marshes before and after the flow-sediment regulation regime in the Yellow River Delta, China. J Hydrol 450–451:244–253

Broekaert JAC (2005) Analytical atomic spectrometry with flames and plasmas, 2nd edn. Wiley-VCH, Weinheim

Chai MW, Shi FC, Li RL, Qiu GY, Liu FC, Liu LM (2014) Growth and physiological responses to copper stress in a halophyte Spartina alterniflora (Poaceae). Acta Physiol Plant 36:745–754

Chen HR (2011) Distribution and potential ecological risk assessment of heavy metals in surface sediments of Luoyuan bay. J Fujian Fish 33: 45–49 (in Chinese)

Chen S, Torres R (2012) Effects of geomorphology on the distribution of metal abundance in the salt marsh sediment. Estuar Coasts 35:1018–1027

Cheng P, Gao S, Li XS (2001) Evaluation of a wide range laser particle size analyses and comparison with pipette and sieving methods. Acta Sedimentol Sin 19:449–455 (in Chinese)

Dietz R, Outridge PM, Hobson KA (2009) Anthropogenic contributions to mercury levels in present-day Arctic animals—a review. Sci Total Environ 407:6120–6131

Du Laing G, Vandecasteele B, Rinklebe J, Meers E, Tack FMG (2009) Trace metal behaviour in estuarine and riverine floodplain soils and sediments: a review. Sci Total Environ 407:3972–3985

Duarte B, Caetano M, Almeida PR, Vale C, Cacador I (2010) Accumulation and biological cycling of heavy metal in four salt marsh species, from Tagus estuary (Portugal). Environ Pollut 158: 1661–1668

Fang TH, Li JY, Feng HM, Chen HY (2009) Distribution and contamination of trace metals in surface sediments of the East China Sea. Mar Environ Res 68:178–187

Fang SB, Jia XB, Yang XY, Li YD, An SQ (2012) A method of identifying priority spatial patterns for the management of potential ecological risks posed by heavy metals. J Hazard Mater 237–238:290–298

Feng H, Han X, Zhang W, Yu L (2004) A preliminary study of heavy metal contamination in Yangtze River intertidal zone due to urbanization. Mar Pollut Bull 49:910–915

Gao WH, Du YF, Wang DD, Gao S (2012) Distribution patterns of heavy metals in surficial sediment and their influence on the environment quality of the intertidal flat of Luoyuan Bay, Fujian coast. Environ Sci 33:3097–3103 (in Chinese)

Gao S, Du YF, Xie WJ, Gao WH, Wang DD, Wu XD (2014) Environment-ecosystem dynamic processes of *Spartina alterniflora* salt-marshes along the eastern China coastlines. Sci China Earth Sci 57:2567–2586

Garcia-Tarrason M, Pacho S, Jover L, Sanpera C (2013) Anthropogenic input of heavy metals in two Audouin's gull breeding colonies. Mar Pollut Bull 74:285–290

Gomez SR (2013) Bioaccumulation of heavy metals in *Spartina*. Funct Plant Biol 40:913–921

Han YM, Du PX, Cao JJ, Posmentier ES (2006) Multivariate analysis of heavy metal contamination in urban dusts of Xi'an, Central China. Sci Total Environ 355:176–186

Horowitz AJ, Elrick KA (1987) The relation of stream sediment surface area, grain size and composition to trace element chemistry. Appl Geochem 2:437–451

Hu BQ, Cui RY, Li J, Wei HL, Zhao JT, Bai FL, Song WY, Ding X (2013) Occurrence and distribution of heavy metals in surface sediments of the Changhua River estuary and adjacent shelf (Hainan Island). Mar Pollut Bull 76:400–405

Li CX, Zhang JQ, Fan DD, Deng B (2001) Holocene regression and the tidal radial sand ridge system formation in the Jiangsu coastal zone, east China. Mar Geol 173:97–120

Li L, Wang YL, Jiang M, Yuan Q, Shen XQ (2012) Analysis of the source, potential biological toxicity of heavy metals in the surface sediments from shellfish culture mudflats of Rudong Country, Jiangsu Province. Environ Sci 33:2607–2613 (in Chinese)

Li FR, Duan LL, Wang FH (2013a) Research progress in heavy metal accumulation of the halophyte *Spartina alterniflora*. J Ecol Environ Sci 22:1263–1268 (in Chinese)

Li GG, Hu BQ, Bi JQ, Leng QN, Xiao CQ, Yang ZC (2013b) Heavy metals distribution and contamination in surface sediments of the coastal Shandong Peninsula (Yellow Sea). Mar Pollut Bull 76:420–426

Liao Y, Huang HJ, Li L, Yuan Q, Jiang M, Shen XQ, Wang YL (2012) Distribution and potential ecological risk assessment of heavy metals in shellfish culture area of Rudong, Jiangsu Province, China. Environ Monit Assess 28:4–9 (in Chinese)

Lin YC, Chang-Chien GP, Chiang PC, Chen WH, Lin YC (2013) Multivariate analysis of heavy metal contaminations in seawater and sediments from a heavily industrialized harbor in Southern Taiwan. Mar Pollut Bull 76:266–275

Liu F, Pang S, Chopin T, Gao S, Shan T, Zhao X, Li J (2013) Understanding the recurrent large-scale green tide in the Yellow Sea: temporal and spatial correlations between multiple geographical, aquacultural and biological factors. Mar Environ Res 83:38–47

Lu RK (2000) Soil agricultural chemistry analytical method. China Agriculture Press, Beijing

Maanan M, Landesman C, Maanan M, Zourarah B, Fattal P, Sahabi M (2013) Evaluation of the anthropogenic influx of metal and metalloid contaminants into the Moulay Bousselham lagoon, Morocco, using chemometric methods coupled to geographical information systems. Environ Sci Pollut Res 20:4729–4741

Müller G (1979) Schwermetalle in den sedimenten des Rheins-Veränderungen seit 1971. Umschau 79:778–783

Pisani O, Oros DR, Oyo-Ita OE, Ekpo BO, Jaffe R, Simoneit BRT (2013) Biomarkers in surface sediments from the Cross River and estuary system, SE Nigeria: assessment of organic matter sources of natural and anthropogenic origins. Appl Geochem 31:239–250

Prasad MNV (1997) Trace metals. In: Prasad MNV (ed) Plant ecophysiology. Wiley, New York, pp 207–249

Prosi F (1989) Factors controlling biological availability and toxic effects of lead in aquatic organisms. Sci Total Environ 79:157–169

Ren ME (1986) The bulletin of coastal zone and tidal flat resources survey in Jiangsu Province. China Ocean Press, Beijing

Retnam A, Zakaria MP, Juahir H, Aris AZ, Zali MA, Kasim MF (2013) Chemometric techniques in distribution, characterization and source apportionment of polycyclic aromatic hydrocarbons (PAHS) in aquaculture sediments in Malaysia. Mar Pollut Bull 69:55–66

Sinex SA, Wright DA (1988) Distribution of trace metals in the sediments and biota of Chesapeake Bay. Mar Pollut Bull 19:425–431

Singh KP, Malik A, Sinha S (2005) Water quality assessment and apportionment of pollution sources of Gomti River (India) using multivariate statistical techniques—a case study. Anal Chim Acta 538: 355–374

Song Y, Xie SD, Zhang YH, Zeng LM, Salmon LG, Zheng M (2006) Source apportionment of PM2.5 in Beijing using principal component analysis/absolute principal component scores and UNMIX. Sci Total Environ 372:278–286

Sun J, Gu XY, Zhang AQ, Wang XR (2010) Organism qualities and pollution assessment at the Yellow Sea of Jiangsu Province. Mar Sci 34:28–33 (in Chinese)

Thurston GD, Spengler JD (1985) A quantitative assessment of source contributions to inhalable particulate matter pollution in metropolitan Boston. Atmos Environ 19:9–25

Tomsett AB, Thurman DA (1988) Molecular biology of metal tolerance of plants. Plant Cell Environ 11:383–394

Wan YS, Zhang QN (1985) The source and movement of sediments of radiating sand ridges off Jiangsu coast. Oceanol et Limnol Sin 16: 392–399 (in Chinese)

Wang AJ, Ye X (2013) Erosion and deposition processes of cohesive sediment in *Spartina alterniflora* marsh, Luoyuan Bay in the north of Fujian coast, China. Quat Sci 33:582–593 (in Chinese)

Wang Y, Zhu DK (1990) Tidal flats of China. Quat Sci 4:291–300 (in Chinese)

Wang DD, Gao S, Du YF, Gao WH (2012) Distribution patterns of sediment chlorophyll-*a* in *Spartina alterniflora* salt marshes at Rudong coast of Jiangsu, East China. Chin J Ecol 31:2247–2254 (in Chinese)

Wang SL, Xu XR, Sun YX, Liu JL, Li HB (2013a) Heavy metal pollution in coastal areas of South China: a review. Mar Pollut Bull 76:7–15

Wang AJ, Ye X, Li YH (2013b) Environmental dynamic mechanisms for sediment erosion and accretion over embayment coastal wetland during typhoon event: a case study from Luoyuan Bay, China. Acta Sedimentol Sin 31:315–324 (in Chinese)

Williams TP, Bubb JM, Lester JN (1994) Metal accumulation within salt marsh environments: a review. Mar Pollut Bull 28:277–290

Yu D (2013) Correlation analysis and countermeasure research of Luoyuan Bay heavy metal environment with coastal industrial layout. Dissertation, Dalian Maritime University, China

Zhang J (1995) Geochemistry of trace metals from Chinese river/estuary systems: an overview. Estuar Coast Shelf Sci 41:631–658

Zhang B (2010) Study on spatial variability and assessments of soil nutrients and heavy metals intertidal zones. Dissertation, Nanjing Agricultural University, China

Zhang J, Liu CL (2002) Riverine composition and estuarine geochemistry of particulate metals in China—weathering features, anthropogenic impact and chemical fluxes. Estuar Coast Shelf Sci 54:1051–1070

Zhang CS, Wang LJ, Li GS, Dong SS, Yang JG, Wang XL (2002) Grain size effect on multi-element concentrations in sediments from the intertidal flats of Bohai Bay, China. Appl Geochem 17:59–68

Zhang WG, Feng H, Chang J, Qu JG, Xie HX, Yu LZ (2009) Heavy metal contamination in surface sediments of Yangtze River intertidal zone: an assessment from different indexes. Environ Pollut 157: 1533–1543

Zhang B, Zheng QS, Zhao GM, Liu ZP (2011) Pollution assessments on heavy metals in sediment in inter-tidal aqua-farm area based on GIS and geostatistics. Mar Environ Sci 30:376–379 (in Chinese)

Zhang R, Zhang F, Ding YJ, Gao JR, Chen J, Zhou L (2013) Historical trends in the anthropogenic heavy metal levels in the tidal flat sediments of Lianyungang, China. J Environ Sci 25:1458–1468

Zhang LH, Du YF, Wang DD, Gao S, Gao WH (2014) Distribution patterns and pollution assessments of heavy metals in the *Spartina alterniflora* salt-marsh wetland of Rudong, Jiangsu Province. Environ Sci 35:2401–2410 (in Chinese)

Zhao YY, Yan MC (1994) Study method of sediment geochemistry of the China shelf sea. Science press, Beijing, p 203

Zhou YW, Zhao B, Peng YS, Chen GZ (2010) Influence of mangrove reforestation on heavy metal accumulation and speciation in intertidal sediments. Mar Pollut Bull 60:1319–1324